

Dedifferentiation of human Glioma cells by reprogramming confers cancer stem cell properties

Javier Rojo Pérez, Shukry Habib, Dolores Delgado and Ignacio Sancho-Martínez
King's College London and Instituto de Biomedicina y Biotecnología de Cantabria (IBBTec), Santander, Spain.



INTRODUCTION

Cancer stem cells (CSCs) are dedifferentiated malignant cell populations able to initiate and maintain tumour heterogeneity and believed to be able to evade therapy. CSCs have thus emerged as responsible for metastasis and secondary tumor formation, making them an attractive and obligatory therapeutic target. There are two prevailing theories attempting to explain the appearance of stem cells with malignant properties:

- That transforming mutations occur in pre-existent adult stem cell populations already bearing self-renewal and multilineage differentiation properties;
- That cancer progression contributes to the dedifferentiation of transformed somatic cells and their transition towards a stem cell phenotype.

Previous work by my supervisor demonstrated the utility of differentiation platforms, namely the generation of Neural Progenitor Cells (NPCs) from human iPSCs, as a suitable strategy for the study of driver mutations and the mechanistic events underlying adult stem cell transformation towards a cancer stem cell phenotype. However, an alternative mechanism for the generation of CSCs remains unexplored up to date, that is, dynamic reversion processes of transformed differentiated cancer cells.

AIMS AND INNOVATION

Development of novel methodologies for the dedifferentiation of glioma cells and the establishment of human GSCs *in vitro* models based on dynamic reversion mechanisms. To do so I focused on the following aims:

- Establishment of reprogramming methodologies for studying CSC formation by "dynamic reversion".
- Characterization of malignancy and stemness in reprogrammed cancer stem cells.

MATERIALS AND METHODS

1. Lentiviral production

Lentiviral vectors were co-transfected with packaging plasmids (pMDL, Rev and VSVg) in 293T cells using Lipofectamine 2000 (Invitrogen) and then collected 48, 96 and 144 hours after transfection.

2. Flow cytometry analysis

- Cells were harvested using TripLE (Invitrogen), washed once with PBS and further incubated with the corresponding antibodies in the presence of FACS blocking buffer (1xPBS/10%FCS) for 1 hour on ice in the absence of light.

- After incubation, cells were washed thrice with 1 ml of FACS blocking buffer and resuspended in a total volume of 200 μ l.

3. CFSE staining

- Were conducted according to the manufacturer's instructions with a final concentration of 2.5 μ M.
- At the end of each time point CFSE fluorescence intensity was determined by Flow cytometry.

4. RNA isolation and q-PCR

- 1 μ g of DNase1 (Invitrogen) treated total RNA was used for cDNA synthesis using the iScriptTM cDNA synthesis kit for RT-PCR.

- Real-time PCR was performed using the SYBR Green Supermix.

5. ALDH activity

- Was evaluated according to the manufacturer's protocol (Aldefluor kit, Stem Cell Technologies)

6. Cell Culture

- 293T cells cultured in DMEM containing 10% FBS, 2 mM GlutaMAX (Invitrogen), 50 U/ml penicillin and 50 mg/ml streptomycin (Invitrogen).
- HFF were grown in collagen I coated plates (BD biosciences).

7. Boyden chamber migration assay.

- Five different areas of each chamber were randomly selected for photography with 5X objective (Olympus).
- The average cell number/area was calculated for each chamber. Triplicates were performed for each cell line.

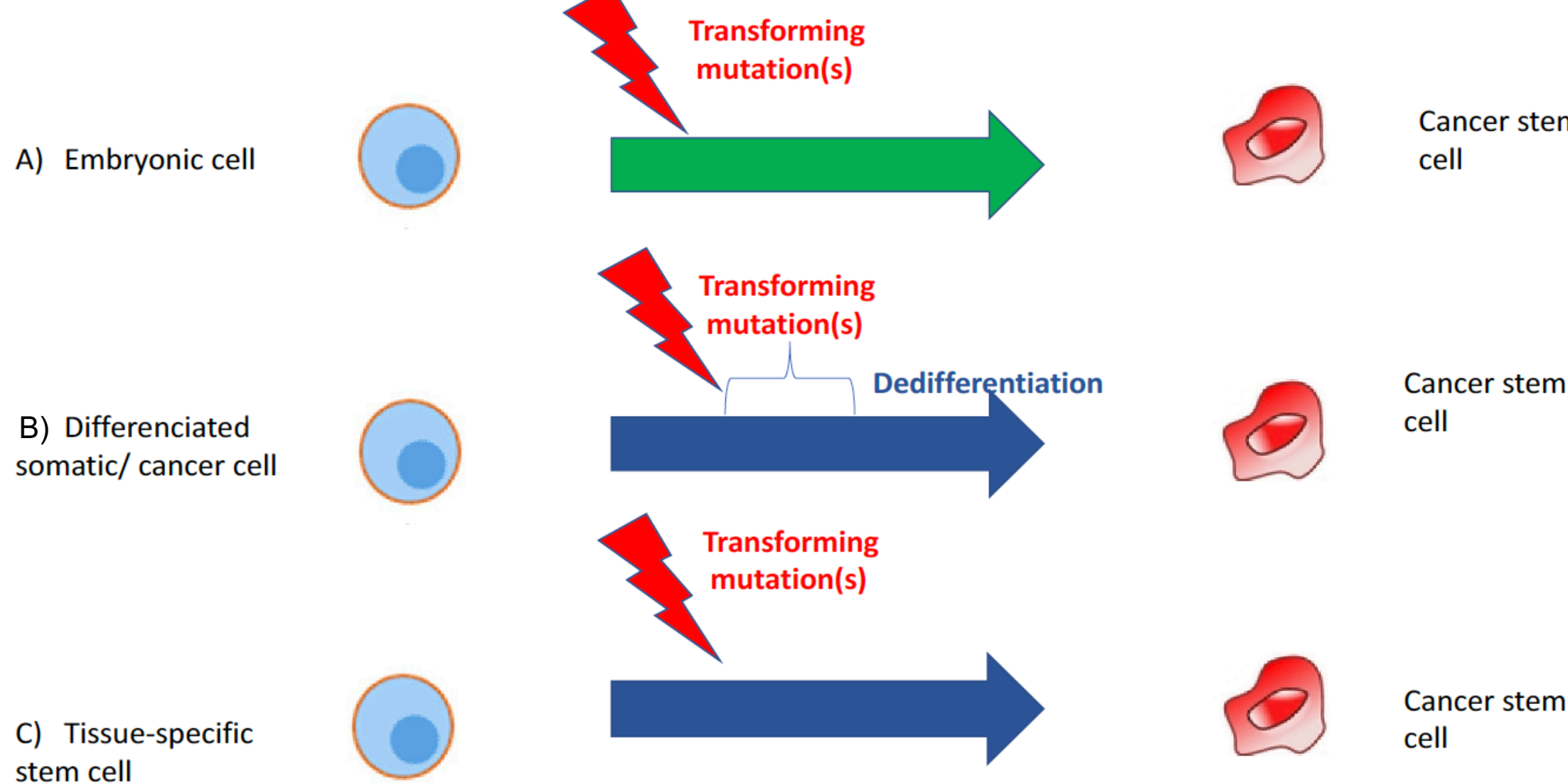
8. Hematoxylin-eosin staining

Tissue sections on positively charged slides were processed by deeping the slides in a series of baths:

- Distilled Water (30s),
- Hematoxylin (5min),
- Distilled water (1min),
- 0.5% Eosin Y (2min),
- 95% Ethanol (30s x2),
- 100% ethanol (30s x2),
- Xylene (30s x2).

9. Immunoblotting

- Cells solubilized in lysis buffer (50 mM Tris-HCl (pH 7.4), 10% Glycerol, 1% (v/v) Triton X-100, 100 mM NaCl, 0.5 mM MgCl₂, 1 mM Na₃VO₄, 10 μ g/ml aprotinin, 1 mM PMSF, 1mM pepstatin, and leupeptin),
- Resulting lysates centrifuged at 16,000 \times g for 15 minutes at 4 $^{\circ}$ C



RESULTS AND DISCUSSION

1) Lentiviral production optimization

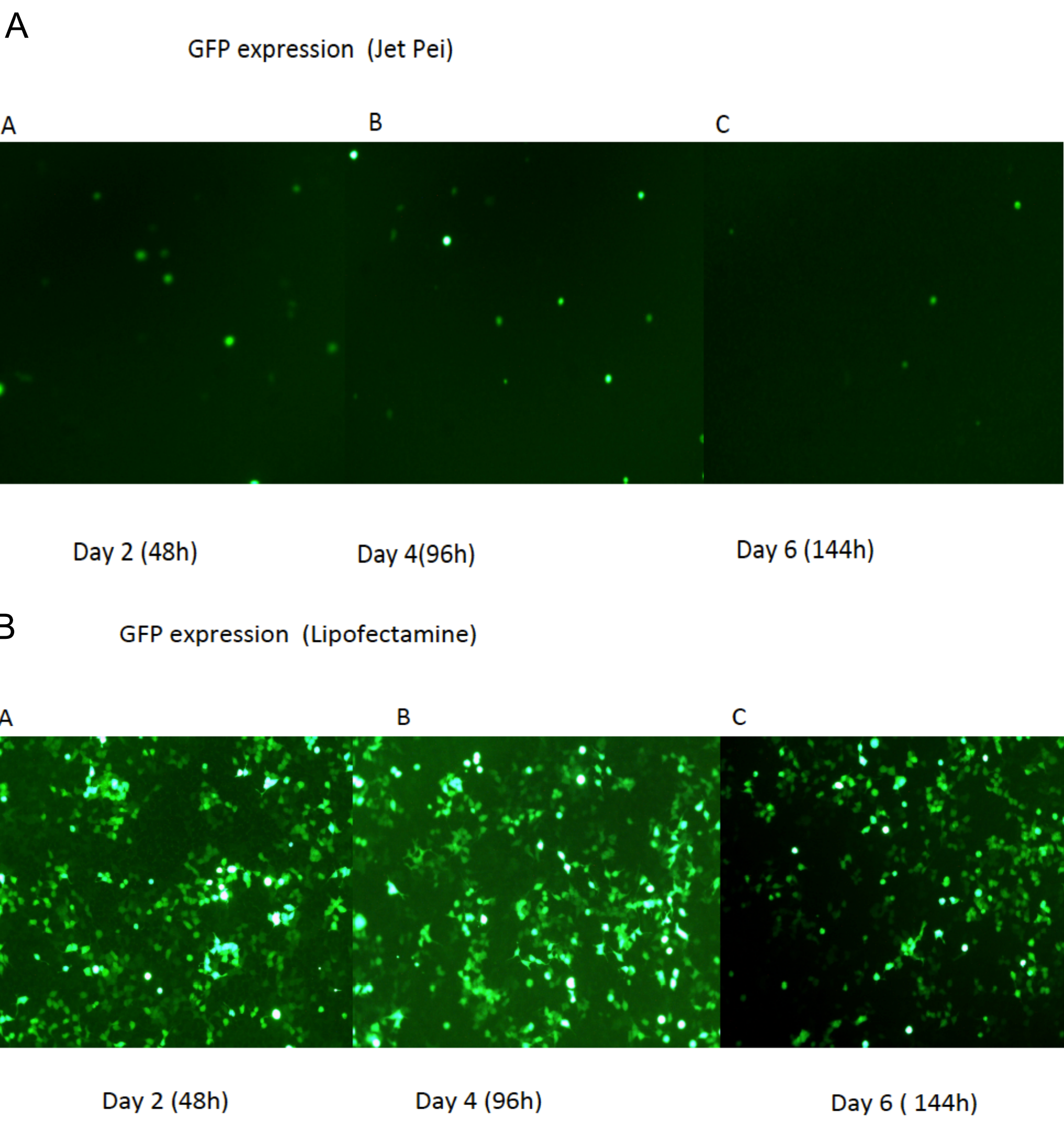


Figure 1: Green fluorescence during lentivirus production via a) Jet-Pei and b) Lipofectamine.

- Green fluorescence of HEK-293t cells 48 hours after transfection.
- Green fluorescence of HEK-293t cells 96 h after transfection.
- Green fluorescence of HEK-293t cells 144 hours after transfection.

2) Reprogramming of glioma cells leads to a dedifferentiated, stem-like signature

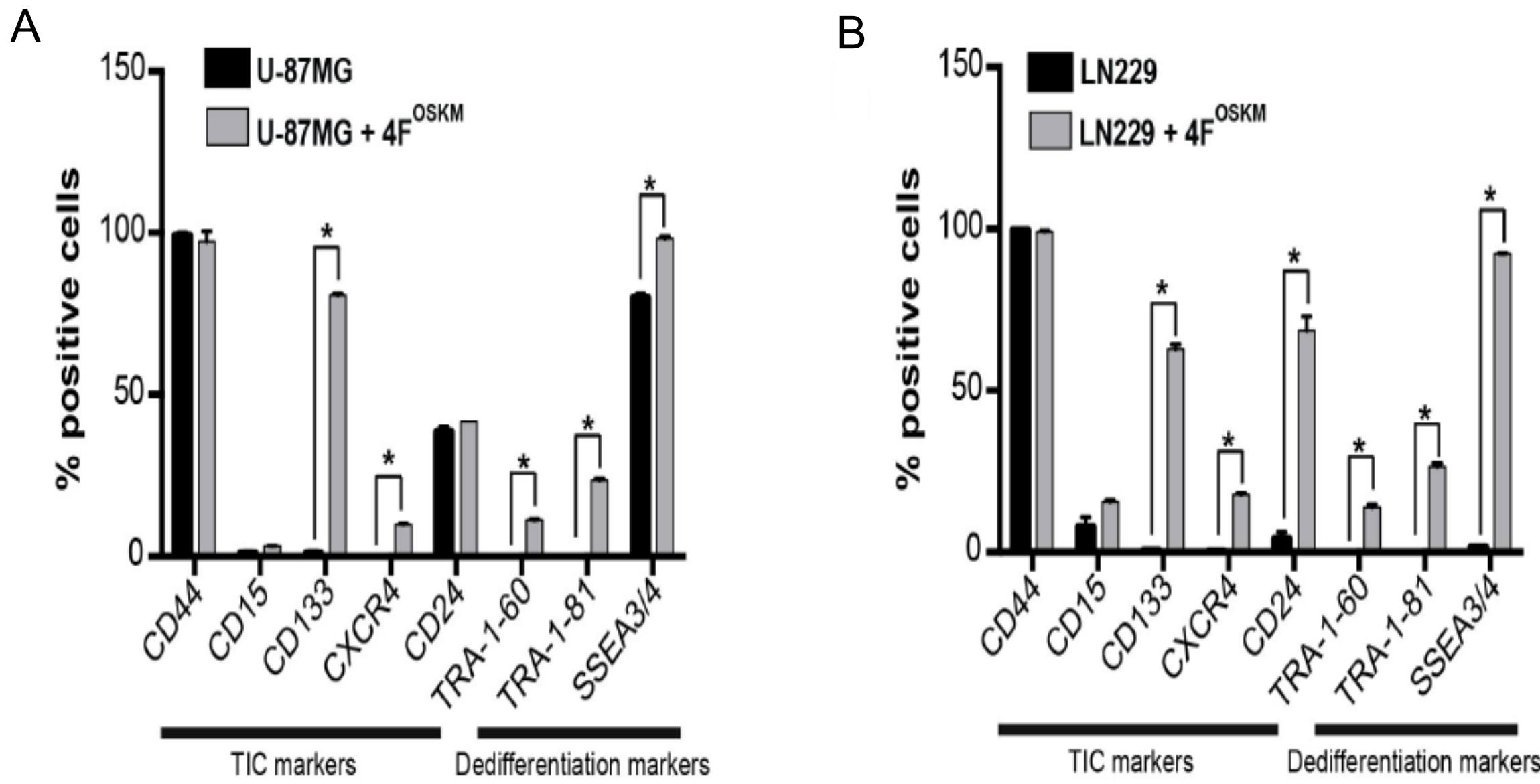


Figure 2: Dedifferentiation of Glioma cells leads to the acquisition of stem cell-like properties.

- Flow Cytometry quantification showing the percentage of cells expressing the indicated markers in parental and dedifferentiated U87MG cells.
- Flow Cytometry quantification showing the percentage of cells expressing the indicated markers in parental and dedifferentiated LN229 cells. Data are represented as mean \pm SD. * p <0.05, n >3.

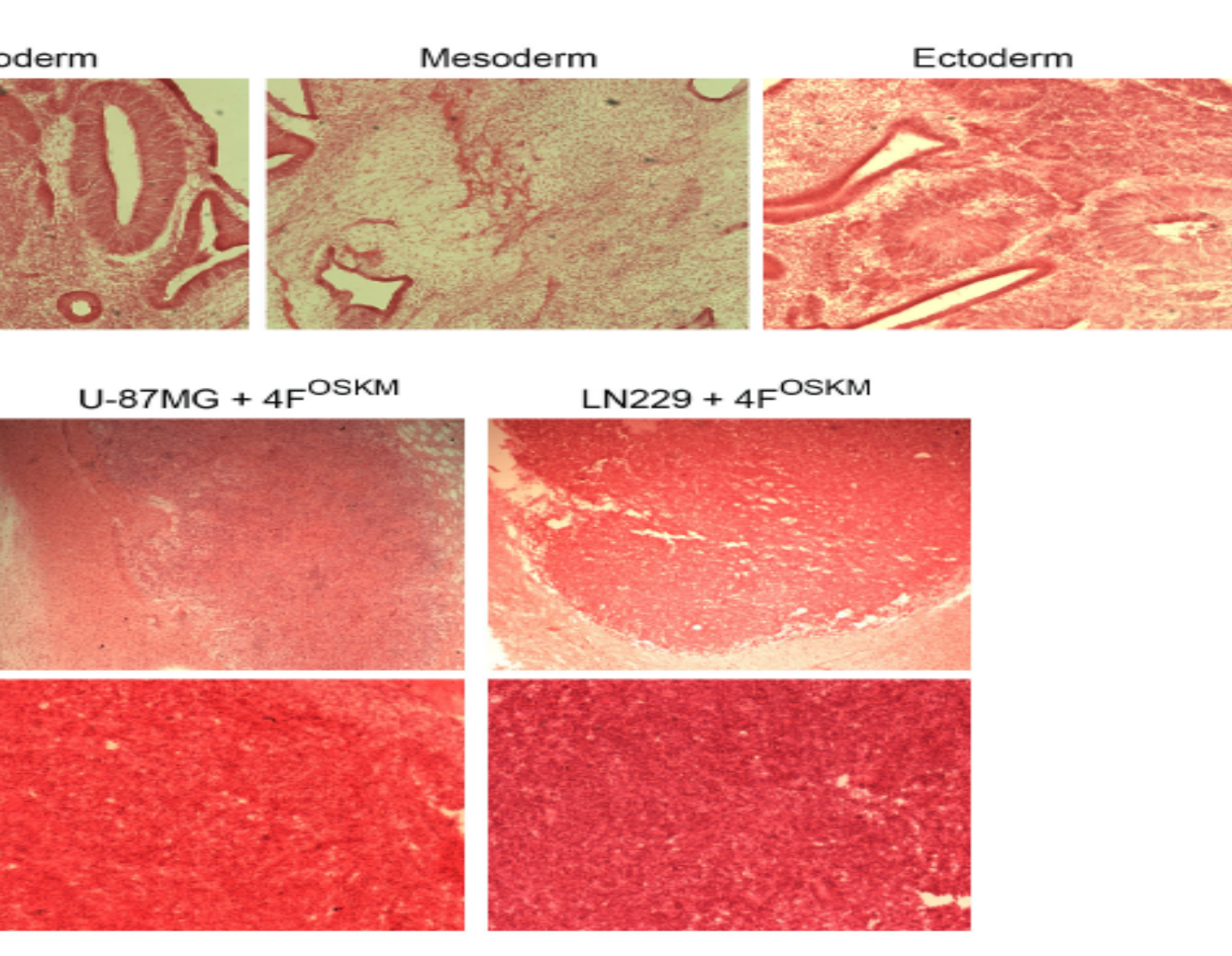
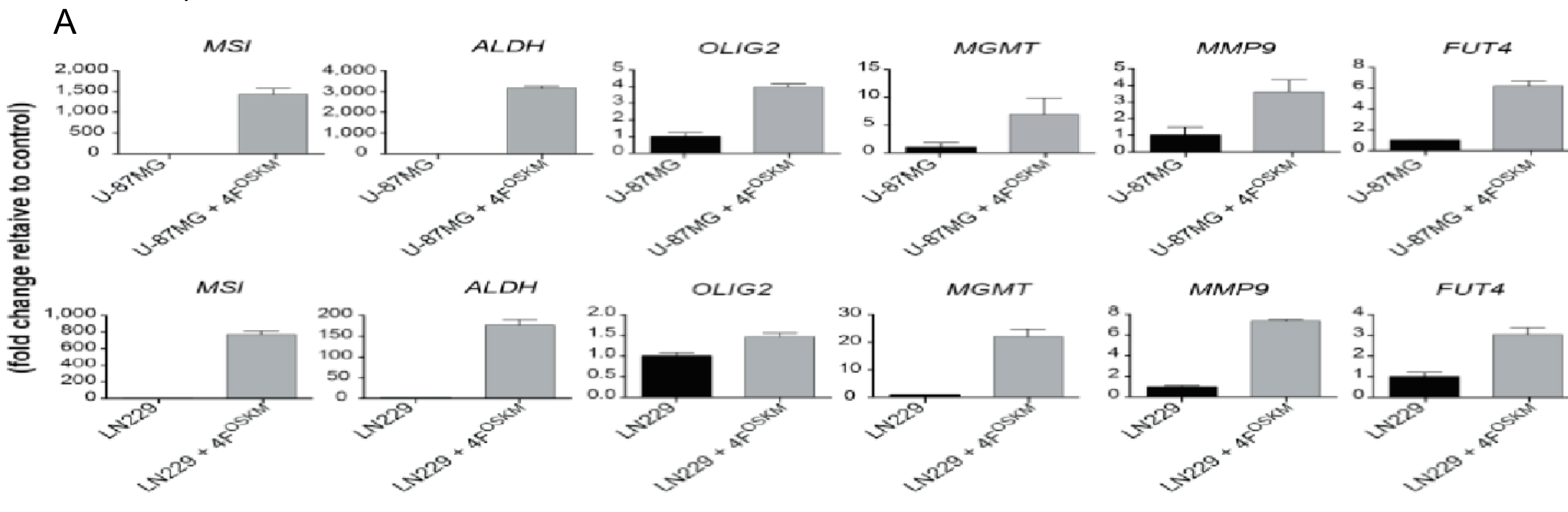


Figure 3: Reprogramming of Glioma cells results in the acquisition of Glioma stem cell properties

- Hematoxylin-Eosin staining highlighting the presence of well-defined teratomas upon injection of undifferentiated iPSCs into the murine brain.
- Hematoxylin-Eosin staining demonstrating the presence of highly aggressive Glioma tumours upon injection into the murine brain.

Figure 4: Dedifferentiation of Glioma cells leads to the acquisition of stem cell-like properties.

- mRNA fold change of glioma stem cell markers in U87MG (upper panels) and LN229 (lower panels) cells before and after dedifferentiation. Data are represented as mean \pm SD. * p <0.05, n >3.

3) Dedifferentiated glioma cells display glioma stem cell-like properties

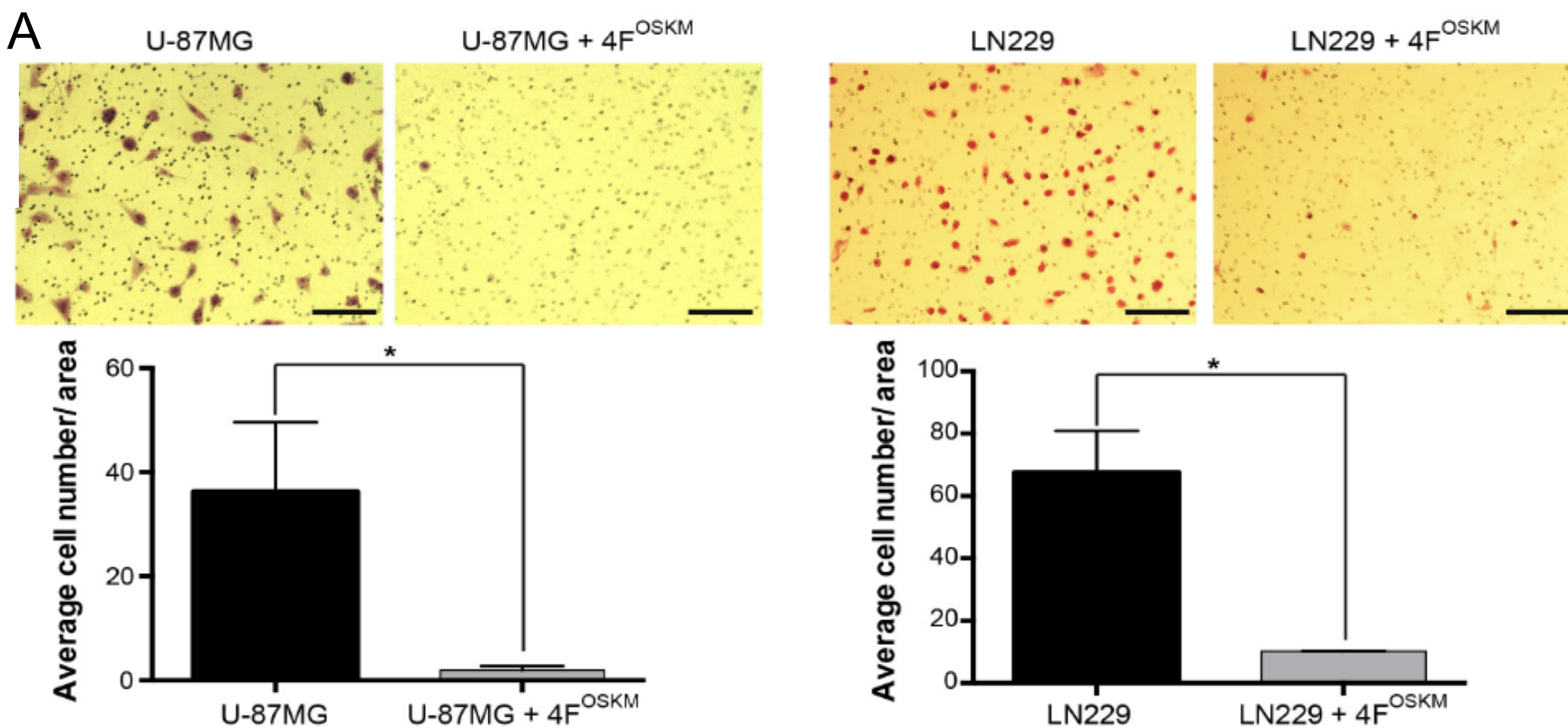


Figure 5: Oncogenic transformation results in dedifferentiation of human iPSC-derived NPCs.

- Two-chamber migration assays demonstrating the acquisition of a quiescent phenotype *in vitro* in the dedifferentiated Glioma cells. On the upper panels, representative pictures of themigrated cells. On the right, quantification of migrated cells for the indicated lines.
- CFSE cell proliferation assays demonstrate comparable proliferation rates before and after reprogramming. Data are represented as mean \pm SD. * p <0.05, n >3.

4) Reprogramming of glioma cells induces metabolic changes

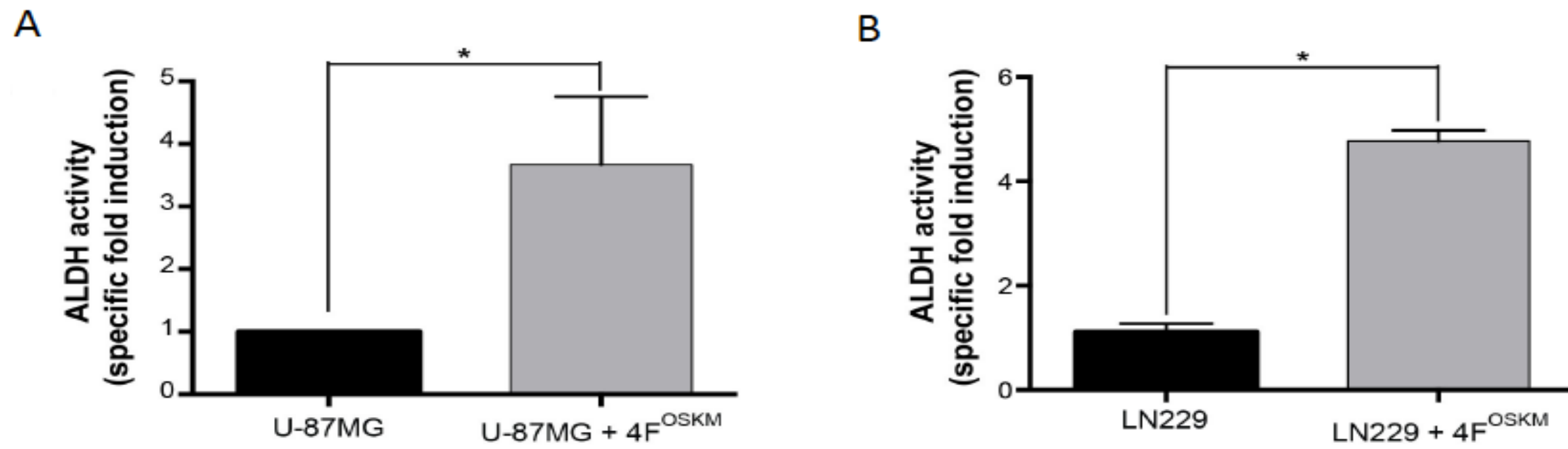


Figure 6: Dedifferentiation of glioma cells induces metabolic changes.

- ALDEFluor assays demonstrating the upregulation of ALDH activities in dedifferentiated U87MG (A) and LN229 (B) Glioma cells. Data are represented as mean \pm SD. * p <0.05, n >3.

CONCLUSION

- Controlled reprogramming upon overexpression of Oct4, SOX2, c-MYC and KLF4, allows for the dedifferentiation of glioma cells to multipotent glioma stem cells in the absence of iPSC generation.
- Dedifferentiation to glioma stem-like cells resulted in increased malignancy and metabolic reprogramming.
- This report represents the initial steps towards the development of reliable platforms for studying dynamic reversion mechanisms underlying CSC generation.
- Modelling cancer by reprogramming approaches provide comprehensive platforms for the identification of the mechanisms driving cancer stem cell generation and cancer cell plasticity.
- Understanding the dynamic mechanisms controlling the dedifferentiation of cancer cells to stem cell phenotypes enlight the basic biology of CSCs and allow for the development of novel therapeutics targeting glioma stem cells.

FUTURE APPROCHES

- Further characterizing the models developed here and utilised such CSC models for understanding CSC differentiation and susceptibility to therapy. Ultimately, my future aims are as follows:
- In vivo analysing the acquisition of multi-lineage differentiation properties upon dedifferentiation of glioma cells to GSCs.
- In vivo role of WNT signalling in Glioma and Glioma Stem Cells.

REFERENCES

- Pulecio, J., Nivet, E., Sancho-Martinez, I., Vitaloni, M., Guenecche, G., Xia, Y., Kurian, L., Dubova, I., Bueren, J., Laricchia-Robbio, L., et al. (2014). Conversion of human fibroblasts into monocyte-like progenitor cells. *Stem Cells* 32, 2923-2938.
- Funato, K., Major, T., Lewis, P.W., Allis, C.D., and Tabar, V. (2014). Use of human embryonic stem cells to model pediatric gliomas with H3.3K27M histone mutation. *Science* 346, 1529-1533.

ACKNOWLEDGEMENTS

I would like to thank Dolores Delgado, Shukry Habib and Ignacio Sancho-Martínez for giving me the opportunity to work alongside them and for all the help, patience, trust and comprehension that they have provide me.